ACS OMEGA

http://pubs.acs.org/journal/acsodf

Article

Formation of Brightly Luminescent MoS_2 Nanoislands from Multilayer Flakes via Plasma Treatment and Laser Exposure

Bo Wang, Sisi Yang, Yu Wang, Younghee Kim, Han Htoon, Stephen K. Doorn, Brendan J. Foran, Adam W. Bushmaker, David R. Baker, Gregory T. Forcherio, and Stephen B. Cronin*

Cite This: https://dx.doi.org/10.1021/acsomega.0c02753

Read Online

ABSTRACT: A robust and reliable method for enhancing the photoluminescence (PL) of multilayer MoS_2 is demonstrated using an oxygen plasma treatment process followed by laser exposure. Here, the plasma and laser treatments result in an indirect-to-direct band gap transition. The oxygen plasma creates a slight decoupling of the layers and converts some of the MoS_2 to MoO_3. Subsequent laser irradiation further oxidizes the MoS_2 to MoO_3, as confirmed via X-ray photoelectron spectroscopy, and results in localized regions of brightly luminescent MoS_2 monolayer triangular islands as seen in high-resolution transmission electron microscopy images. The PL lifetimes are found to decrease from 494 to 190 ps after plasma and laser treatment, reflecting the smaller size of the MoS_2 grains/regions. Atomic force microscopic imaging shows a 2 nm increase in thickness of the laser-irradiated regions, which provides further evidence of the MoS_2 being converted to MoO_3.

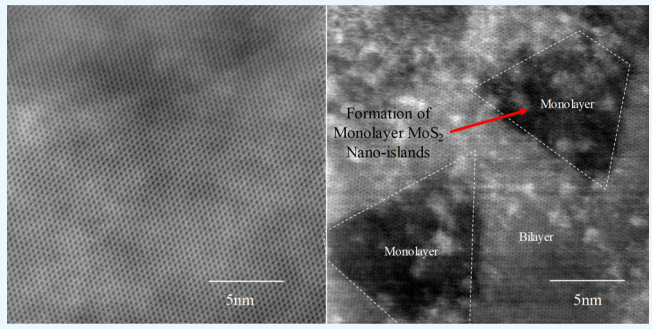

1. INTRODUCTION

Since 2010, intense research in the optical and optoelectronic properties of two-dimensional (2D) transition metal dichalcogenides (TMDCs) has led to great advancements in the materials preparation,[1−9] processing,[10−13] and devices.[10,14−19] Many interesting physical phenomena are seen in these 2D materials, including lasing from monolayer MoS_2 deposited in photonic crystal cavities[20,21] and interlayer excitons bound at the interface between WSe_2 and $MoSe_2$.[22−26] While this intriguing class of materials presents new degrees of freedom in the design and optimization of optoelectronic devices, their extremely high surface-to-volume ratio makes them particularly sensitive to defects, surface contaminants, and other extraneous perturbations from the underlying substrate and environment.[27−29] As such, post processing techniques are needed to mitigate these potential problems and, in general, provide a more robust material platform for reliable device fabrication.

Several techniques have been developed to treat MoS_2 flakes in order to increase their photoluminescence (PL) efficiency. Amani et al. reported that treatment with an organic superacid can uniformly enhance the PL and minority carrier lifetime of monolayer MoS_2 flakes with "near unity" quantum efficiency.[18] Mouri et al. reported that chemical-doped monolayer MoS_2 flakes can show tunable and enhanced PL by changing the doping level of the doped MoS_2 flakes.[30] Our group reported both oxygen plasma-based and proton irradiation-based treatment of multilayer MoS_2 flakes that show stable direct band gap transitions and significantly enhanced PL efficiencies.[8,27,28] In 2016, we reported that the PL intensity from multilayer $MoSe_2$ flakes can be enhanced through selective oxidation of one MoS_2 layer.[31] Nan et al. reported substantial enhancements in the PL intensity from monolayer MoS_2 via chemical adsorption of oxygen at defect sites and high-temperature annealing, which provides an efficient mechanism for converting trions to radiative excitons.[32] Kang et al. reported PL quenching in single-layer MoS_2 via oxygen plasma treatment.[33]

While previous studies have investigated the effects of plasma treatment and chemisorption, here, we combine an oxygen plasma treatment with subsequent laser exposure to achieve a new state of the material system that is not achievable with the plasma alone or the laser alone. Using high-resolution transmission electron microscopy (HRTEM), we observe the emergence of triangular regions of monolayer MoS_2 (i.e., nanoislands) in the two-step process, which are highly luminescent. This approach enables patterning of specific regions of the TMDC material by the selective exposure to light. Several control experiments are carried out to understand the role of each step of the treatment (i.e., O_2

Received: June 11, 2020
Accepted: July 23, 2020

plasma vs laser exposure) in the MoS_2-to-MoO_3 transformation.

2. RESULTS AND DISCUSSION

In the sample preparation process, crystalline MoS_2 is first mechanically exfoliated onto transparent polydimethylsiloxane. Based on the indirect band peak from PL spectra, once an MoS_2 flake of the desired size and thickness is located via optical microscopy, the flake is transferred using a home-built contact aligner (i.e., dry transfer method) with a 50× objective lens onto a transmission electron microscopy (TEM)-compatible silicon nitride substrate.[34] The flakes are then treated with a remote oxygen plasma for 3 min using an XEI Evactron Soft Clean plasma cleaner, in which the plasma is generated from room air flowing past a 15 W RF source at 200 mTorr. The flake is placed 10 cm downstream from the oxygen plasma source. In this remote configuration, the radical species lose most of their kinetic energy but still remain chemically reactive. The flake is then exposed to laser irradiation in ambient air using a 532 nm CW laser focused through a 100× (0.86 NA) objective lens to a beam of approximately 1 μm size and intensity of 3.5 mW/μm^2. PL spectra were collected from these MoS_2 flakes before and after the plasma/laser treatment using an inVia micro-spectrometer (Renishaw, Inc.) using a 532 nm-wavelength laser with a power density of 0.03 mW/μm^2, which is 2 orders of magnitude weaker than the laser exposure treatment and, thus, does not change the material during the PL measurements. X-ray photoelectron spectroscopy (XPS) was performed using a 10 μm spot size on a ULVAC PHI VersaProbe III (Physical Electronics, East Chanhassen, MN, USA) with a monochromated Al Kα source on the MoS_2 flakes before the treatment, after plasma treatment, and after the plasma and laser treatment. Atomic force microscopy (AFM) images of the laser-exposed regions in the MoS_2 were taken using dimension ICON AFM (Bruker, Inc.). Time-resolved PL (TRPL) spectra were taken from the MoS_2 flakes before the treatment, after plasma treatment, and after the plasma and laser treatment and were carried out on a laser scanning confocal optical microscope using a 50 fs pulsed 405 nm diode laser with a pump power of <60 nW and repetition rate of 20 MHz. The TRPL spectra were detected using single-photon avalanche photodiodes (SPCM-AQR-14, PerkinElmer) connected to a HydraHarp 400 (PicoQuant) time-correlated single-photon counting system. To rule out laser-induced heating effects, we have included results in the Supporting Information taken from a MoS_2 flake that was thermally annealed in an argon environment at 500 °C for 1 h, immediately following the plasma treatment.

Figure 1a shows a TEM image of a suspended MoS_2 bilayer, which is treated by oxygen plasma only. In this TEM image, we are able to clearly see the atomic lattice structure, which is almost the same as an untreated bilayer MoS_2 flake. Figure 1b shows a TEM image of a suspended MoS_2 bilayer after plasma and laser treatment, showing the formation of triangular and trapezoidal nanoislands, which is indicated by the different contrast (i.e., the difference in energy loss of the electron beam) of the TEM images, in this two-step process (i.e., plasma followed by laser exposure). Here, the nanoislands of the monolayer material are embedded within the bilayer MoS_2, indicating the partial conversion of one of the MoS_2 layers to MoO_3, which is consistent with the XPS data described below. It is also apparent from these images that the light-induced oxidation of the MoS_2 material follows the axes of the crystal,

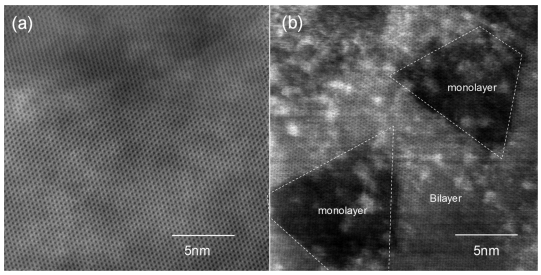

Figure 1. TEM images of MoS_2: (a) oxygen plasma-treated only and (b) oxygen plasma-treated and laser-exposed.

forming triangular patterns. These resulting monolayer nanoislands of MoS_2 are more than 1 order of magnitude more luminescent than the original bilayer material.

Figure 2a shows the PL spectra of bilayer MoS_2 (indicated by the position of the indirect band gap emission) taken before

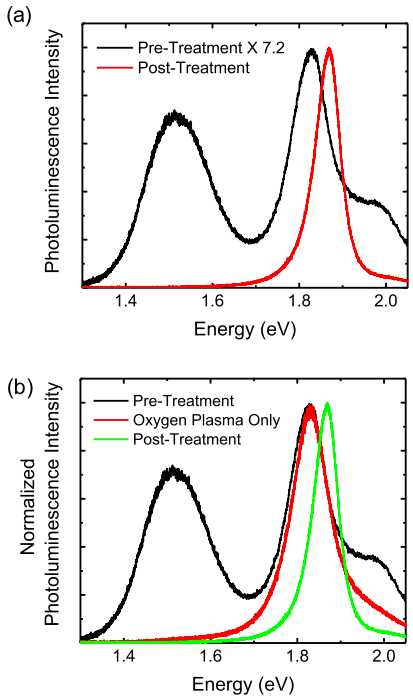

Figure 2. (a) PL spectra for a bilayer MoS_2 flake before and after plasma treatment and laser exposure. (b) Normalized PL spectra for the same bilayer MoS_2 flake taken before treatment, after oxygen plasma treatment only, and after oxygen plasma treatment and laser exposure.

and after plasma and laser exposure. Here, we see a 7.2-fold increase in the peak PL intensity after the treatment with a 22% linewidth narrowing and complete suppression of the indirect band gap transition. Figure 2b shows the PL spectra taken before treatment, after a 3 min oxygen plasma exposure only, and after a 3 min oxygen plasma and a 3 min laser exposure. Here, the effect of the laser exposure is to increase the energy (i.e., 40 meV blue shift from 1.83 to 1.87 eV) of the direct band gap emission, while the PL intensity remains unchanged. The laser exposure also produces a narrower distribution (98.5 to 65.5 meV) and a decreased lifetime of the ground-state exciton. As a control experiment, two few-layer MoS_2 flakes were thermally annealed at 500 °C in argon gas at a flow rate at 1 SLM after the plasma treatment step instead of

https://dx.doi.org/10.1021/acsomega.0c02753
ACS Omega XXXX, XXX, XXX−XXX

laser exposure. These results are shown in Figure S1 of the Supporting Information. We find PL intensity to be an order of magnitude weaker after thermally annealed flakes, indicating that the transition to MoO_3 with MoS_2 islands is a photodriven rather than thermally driven process with oxygen plasma-treated MoS_2 flakes.

Figure 3 shows XPS spectra of a 10 μm diameter region of multilayer MoS_2 flakes taken before and after plasma and laser exposures. Figure 3a shows the Mo 3d spectrum taken before treatment, where we observe Mo $3d_{3/2}$, Mo $3d_{5/2}$, and S 2s states that are consistent with stoichiometric MoS_2.[35] After oxygen plasma treatment, we observe two additional peaks that correspond to the MoO_3 doublet (i.e., MoO_3 $3d_{3/2}$ and MoO_3 $3d_{5/2}$ states), as indicated in Figure 2b.[35−38] Based on these spectra, we believe that we have created subregions of MoO_3 within the MoS_2. Figure 3c shows the Mo 3d spectrum taken after oxygen plasma and a 60 s laser exposure. The MoO_3 contribution becomes more prominent, increasing from 31% of the total Mo $3d_{5/2}$ counts in Figure 2b to 65% in Figure 3c, indicating an additional transformation of MoS_2 to MoO_3.

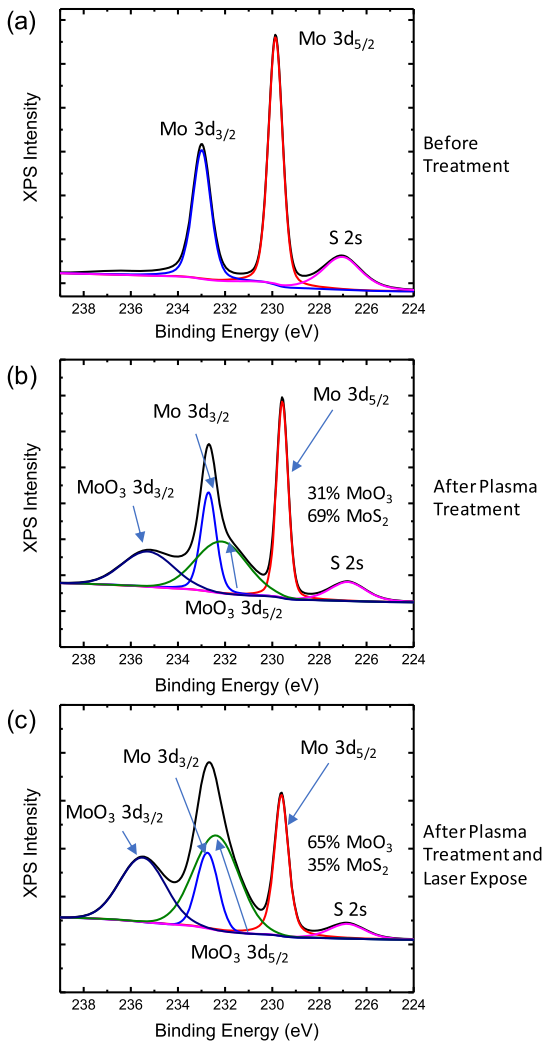

Figure 3. XPS spectra for (a) untreated, (b) oxygen plasma-treated only, and (c) oxygen plasma-treated and laser-exposed bilayer MoS_2 flakes.

Figure S2 of the Supporting Information shows optical microscopy and AFM images of a few-layered MoS_2 flake after plasma treatment and laser exposure, showing an increase in thickness of 2 nm in the region that had undergone laser exposure. This increase in thickness is consistent with the formation of MoO_3, which has a larger thickness than MoS_2.[39,40]

Figure 4 shows the result of PL lifetime measurements taken from treated and untreated MoS_2 flakes with the same thickness (i.e., number of layers). Here, the PL lifetime decreases after oxygen plasma treatment and laser exposure. The time-dependent PL intensities were fitted to biexponential decays, as indicated in the figure. The first decay decreases from 494 ps before treatment to 190 ps after treatment. Here, the plasma-only treatment shows almost no effect on the PL

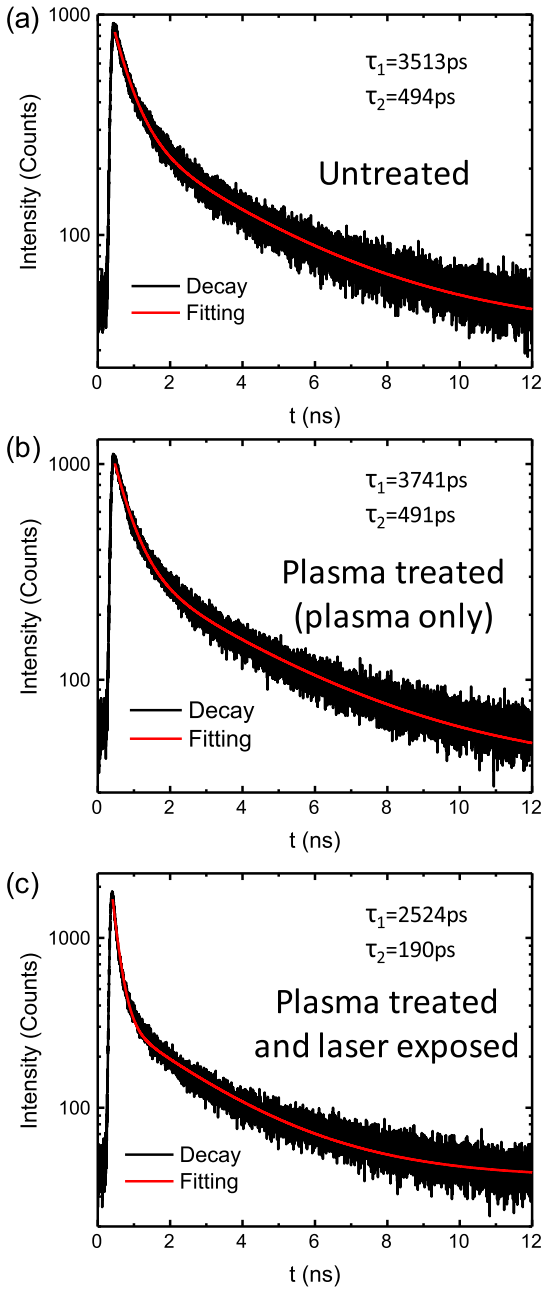

Figure 4. TRPL intensity for (a) untreated, (b) oxygen plasma-treated only, and (c) oxygen plasma-treated and laser-exposed MoS_2 flakes.

https://dx.doi.org/10.1021/acsomega.0c02753
ACS Omega XXXX, XXX, XXX−XXX

lifetime. We believe that the formation of small triangular regions of monolayer MoS_2 is primarily responsible for the shortened lifetimes because of the increased surface-to-volume ratio (or more accurately, the perimeter-to-area ratio), that is, nonradiative recombination occurring at the edges of each MoS_2 grain is primarily responsible for the decrease in the PL lifetime.

3. CONCLUSIONS

In conclusion, we report a two-step method for creating "triangular" MoS_2 nano-islands from exfoliated multilayer MoS_2 flakes using a sequence of plasma and light exposure treatments as observed in TEM images. This plasma/laser treatment induces a transition from indirect to direct band gap material, yielding a sevenfold enhancement in the direct band gap emission (at 1.87 eV) and suppression of the indirect emission (around 1.54 eV). Here, a slight spatial decoupling of the layers is created by intercalated O-species from the plasma treatment. The laser subsequently oxidizes exposed regions of the MoS_2 to MoO_3, as confirmed via XPS, which results in localized areas with brightly luminescent monolayer MoS_2 triangular nanoislands embedded in bilayer MoS_2. A 40 meV blue shift is also observed in the direct-gap emission with a 3 min laser exposure with a 33 meV decrease in the linewidth. Furthermore, we observe a decrease in the PL lifetime from 494 to 190 ps after the plasma and laser treatment, suggesting an increased density of monolayer MoS_2 grain boundaries. An increase in flake thickness is observed in the laser-irradiated regions, providing more evidence that the MoS_2 is partially being converted into MoO_3.

■ ASSOCIATED CONTENT

Supporting Information

The Supporting Information is available free of charge at https://pubs.acs.org/doi/10.1021/acsomega.0c02753.

Optical and AFM images, PL spectra, and TEM images taken from multilayer MoS_2 flakes after oxygen plasma and thermal annealing (PDF)

■ AUTHOR INFORMATION

Corresponding Author

Stephen B. Cronin − *Department of Physics and Astronomy, Ming Hsieh Department of Electrical Engineering, and Mork Family Department of Chemical Engineering and Materials Science, University of Southern California, Los Angeles, California 90089, United States;* orcid.org/0000-0001-9153-7687; Email: scronin@usc.edu

Authors

Bo Wang − *Department of Physics and Astronomy, University of Southern California, Los Angeles, California 90089, United States;* orcid.org/0000-0001-7089-6672

Sisi Yang − *Department of Physics and Astronomy, University of Southern California, Los Angeles, California 90089, United States;* orcid.org/0000-0003-0352-833X

Yu Wang − *Mork Family Department of Chemical Engineering and Materials Science, University of Southern California, Los Angeles, California 90089, United States;* orcid.org/0000-0002-0307-1301

Younghee Kim − *Center for Integrated Nanotechnologies, Materials Physics and Applications Division, Los Alamos National Laboratory, Los Alamos, New Mexico 87545, United States;* orcid.org/0000-0002-4499-3783

Han Htoon − *Center for Integrated Nanotechnologies, Materials Physics and Applications Division, Los Alamos National Laboratory, Los Alamos, New Mexico 87545, United States;* orcid.org/0000-0003-3696-2896

Stephen K. Doorn − *Center for Integrated Nanotechnologies, Materials Physics and Applications Division, Los Alamos National Laboratory, Los Alamos, New Mexico 87545, United States;* orcid.org/0000-0002-9535-2062

Brendan J. Foran − *The Aerospace Corporation, El Segundo, California 90245, United States*

Adam W. Bushmaker − *The Aerospace Corporation, El Segundo, California 90245, United States*

David R. Baker − *Sensors and Electron Devices Directorate, U.S. Army Research Laboratory, Adelphi, Maryland 20783, United States;* orcid.org/0000-0002-9930-5183

Gregory T. Forcherio − *Sensors and Electron Devices Directorate, U.S. Army Research Laboratory, Adelphi, Maryland 20783, United States; Electro-Optic Technology Division, Naval Surface Warfare Center, Crane, Indiana 47522, United States;* orcid.org/0000-0001-7668-0215

Complete contact information is available at: https://pubs.acs.org/10.1021/acsomega.0c02753

Notes

The authors declare no competing financial interest.

■ ACKNOWLEDGMENTS

The authors would like to acknowledge support from the Northrop Grumman Institute of Optical Nanomaterials and Nanophotonics (NG-ION^2) (B.W.). This research was supported by the NSF award no. CBET-1905357 (S.Y.), the Department of Energy DOE Award no. DE-FG02-07ER46376 (Y.W.). This work was also carried out in part at the Center for Integrated Nanotechnologies, a U.S. Department of Energy, Office of Science user facility. Y.K., S.K.D., and H.H. acknowledge partial support of the LANL LDRD program and DOE BES FWP# LANLBES22. The portion of the work done at The Aerospace Corporation was funded by the Independent Research and Development Program at The Aerospace Corporation. This work was also accomplished under USARL Cooperative Agreement no. W911NF-17-2-0057 awarded to G.T.F.

■ REFERENCES

(1) Mak, K. F.; Lee, C.; Hone, J.; Shan, J.; Heinz, T. F. Atomically Thin MoS_2: A New Direct-Gap Semiconductor. *Phys. Rev. Lett.* **2010**, *105*, 136805.

(2) Dhall, R.; Li, Z.; Kosmowska, E.; Cronin, S. B. Charge neutral MoS_2 field effect transistors through oxygen plasma treatment. *Jpn. J. Appl. Phys.* **2016**, *120*, 195702.

(3) Xu, X.; Das, G.; He, X.; Hedhili, M. N.; Fabrizio, E. D.; Zhang, X.; Alshareef, H. N. High-Performance Monolayer MoS 2 Films at the Wafer Scale by Two-Step Growth. *Adv. Funct. Mater.* **2019**, *29*, 1901070.

(4) Kim, T.-Y.; Cho, K.; Park, W.; Park, J.; Song, Y.; Hong, S.; Hong, W. K.; Lee, T. Irradiation Effects of High-Energy Proton Beams on MoS2 Field Effect Transistors. *ACS Nano* **2014**, *8*, 2774−2781.

(5) Zhang, C. X.; Newaz, A. K. M.; Wang, B.; Zhang, E. X.; Duan, G. X.; Fleetwood, D. M.; Alles, M. L.; Schrimpf, R. D.; Bolotin, K. I.; Pantelides, S. T. Electrical Stress and Total Ionizing Dose Effects on MoS2 Transistors. *IEEE Trans. Nucl. Sci.* **2014**, *61*, 2862−2867.

(6) Meng, J.; Wang, G.; Li, X.; Lu, X.; Zhang, J.; Yu, H.; Chen, W.; Du, L.; Liao, M.; Zhao, J.; Chen, P.; Zhu, J.; Bai, X.; Shi, D.; Zhang, G. Rolling Up a Monolayer MoS2 Sheet. *Small* **2016**, *12*, 3770−3774.
(7) Lee, J.; Krupcale, M. J.; Feng, P. X. L. Effects of gamma-ray radiation on two-dimensional molybdenum disulfide (MoS2) nanomechanical resonators. *Appl. Phys. Lett.* **2016**, *108*, 023106.
(8) Li, H.; Lu, G.; Wang, Y.; Yin, Z.; Cong, C.; He, Q.; Wang, L.; Ding, F.; Yu, T.; Zhang, H. Mechanical Exfoliation and Characterization of Single- and Few-Layer Nanosheets of WSe2, TaS2, and TaSe2. *Small* **2013**, *9*, 1974−1981.
(9) Ochedowski, O.; Marinov, K.; Wilbs, G.; Keller, G.; Scheuschner, N.; Severin, D.; Bender, M.; Maultzsch, J.; Tegude, F. J.; Schleberger, M. Radiation hardness of graphene and MoS2 field effect devices against swift heavy ion irradiation. *Jpn. J. Appl. Phys.* **2013**, *113*, 214306.
(10) Gao, G.; Yu, J.; Yang, X.; Pang, Y.; Zhao, J.; Pan, C.; Sun, Q.; Wang, Z. L. Triboiontronic Transistor of MoS2. *Adv. Mater.* **2019**, *31*, 1806905.
(11) Ross, J. S.; Wu, S. F.; Yu, H. Y.; Ghimire, N. J.; Jones, A. M.; Aivazian, G.; Yan, J. Q.; Mandrus, D. G.; Xiao, D.; Yao, W.; Xu, X. D. Electrical control of neutral and charged excitons in a monolayer semiconductor. *Nat. Commun.* **2013**, *4*, 1474.
(12) Dhall, R.; Neupane, M. R.; Wickramaratne, D.; Mecklenburg, M.; Li, Z.; Moore, C.; Lake, R. K.; Cronin, S. Direct Band Gap Transition in Many-Layer MoS_2 by Plasma Induced Layer Decoupling *Adv. Mater.* **2015**, *27*, DOI: DOI: 10.1002/adma.201405259.
(13) Rezende, N. P.; Cadore, A. R.; Gadelha, A. C.; Pereira, C. L.; Ornelas, V.; Watanabe, K.; Taniguchi, T.; Ferlauto, A. S.; Malachias, A.; Campos, L. C.; Lacerda, R. G. Probing the Electronic Properties of Monolayer MoS2 via Interaction with Molecular Hydrogen. *Adv. Electron. Mater.* **2019**, *5*, 1800591.
(14) Tsai, D.-S.; Lien, D. H.; Tsai, M. L.; Su, S. H.; Chen, K. M.; Ke, J. J.; Yu, Y. C.; Li, L. J.; He, J. H. Trilayered MoS2 Metal-Semiconductor-Metal Photodetectors: Photogain and Radiation Resistance. *IEEE J. Sel. Top. Quantum Electron.* **2014**, *20*, 30.
(15) Zan, R.; Ramasse, Q. M.; Jalil, R.; Georgiou, T.; Bangert, U.; Novoselov, K. S. Control of Radiation Damage in MoS2 by Graphene Encapsulation. *ACS Nano* **2013**, *7*, 10167−10174.
(16) Stergiou, A.; Tagmatarchis, N. Molecular Functionalization of Two-Dimensional MoS 2 Nanosheets. *Chem.—Eur. J.* **2018**, *24*, 18246−18257.
(17) Tongay, S.; Suh, J.; Ataca, C.; Fan, W.; Luce, A.; Kang, J. S.; Liu, J.; Ko, C.; Raghunathanan, R.; Zhou, J.; Ogletree, F.; Li, J. B.; Grossman, J. C.; Wu, J. Q. Defects activated photoluminescence in two-dimensional semiconductors: interplay between bound, charged, and free excitons. *Sci. Rep.* **2013**, *3*, 2657.
(18) Amani, M.; Lien, D.-H.; Kiriya, D.; Xiao, J.; Azcatl, A.; Noh, J.; Madhvapathy, S. R.; Addou, R.; Kc, S.; Dubey, M.; Cho, K.; Wallace, R. M.; Lee, S.-C.; He, J.-H.; Ager, J. W.; Zhang, X.; Yablonovitch, E.; Javey, A. Near-unity photoluminescence quantum yield in MoS2. *Science* **2015**, *350*, 1065.
(19) Desai, S. B.; Madhvapathy, S. R.; Sachid, A. B.; Llinas, J. P.; Wang, Q.; Ahn, G. H.; Pitner, G.; Kim, M. J.; Bokor, J.; Hu, C.; Wong, H. S. P.; Javey, A. *Science* **2016**, *354*, 99.
(20) Wu, S.; Buckley, S.; Jones, A. M.; Ross, J. S.; Ghimire, N. J.; Yan, J.; Mandrus, D. G.; Yao, W.; Hatami, F.; Vučković, J.; Majumdar, A.; Xu, X. Control of two-dimensional excitonic light emission via photonic crystal. *2D Mater.* **2014**, *1*, 011001.
(21) Wu, S.; Buckley, S.; Schaibley, J. R.; Feng, L.; Yan, J.; Mandrus, D. G.; Hatami, W.; Vučković, J.; Majumdar, A.; Xu, X.; Xu, X. Monolayer semiconductor nanocavity lasers with ultralow thresholds. *Nature* **2015**, *520*, 69−72.
(22) Rivera, P.; Schaibley, J. R.; Jones, A. M.; Ross, J. S.; Wu, S.; Aivazian, G.; Klement, P.; Seyler, K.; Clark, G.; Ghimire, N. J.; Yan, J.; Mandrus, D. G.; Yao, W.; Xu, X. Observation of long-lived interlayer excitons in monolayer MoSe2−WSe2 heterostructures. *Nat. Commun.* **2015**, *6*, 6242.
(23) Nayak, P. K.; Horbatenko, Y.; Ahn, S.; Kim, G.; Lee, J.-U.; Ma, K. Y.; Jang, A.-R.; Lim, H.; Kim, D.; Ryu, S.; Cheong, H.; Park, N.; Shin, H. S. Probing Evolution of Twist-Angle-Dependent Interlayer Excitons in MoSe2/WSe2 van der Waals Heterostructures. *ACS Nano* **2017**, *11*, 4041−4050.
(24) Rigosi, A. F.; Hill, H. M.; Li, Y.; Chernikov, A.; Heinz, T. F. Probing Interlayer Interactions in Transition Metal Dichalcogenide Heterostructures by Optical Spectroscopy: MoS2/WS2 and MoSe2/WSe2. *Nano Lett.* **2015**, *15*, 5033−5038.
(25) Hanbicki, A. T.; Chuang, H.-J.; Rosenberger, M. R.; Hellberg, C. S.; Sivaram, S. V.; McCreary, K. M.; Mazin, I. I.; Jonker, B. T. Double Indirect Interlayer Exciton in a MoSe2/WSe2 van der Waals Heterostructure. *ACS Nano* **2018**, *12*, 4719−4726.
(26) Chen, J.; Bailey, C. S.; Hong, Y.; Wang, L.; Cai, Z.; Shen, L.; Hou, B.; Wang, Y.; Shi, H.; Sambur, J.; Ren, W.; Pop, E.; Cronin, S. B. Plasmon-Resonant Enhancement of Photocatalysis on Monolayer WSe2. *ACS Photonics* **2019**, *6*, 787−792.
(27) Wang, B.; Yang, S.; Chen, J.; Mann, C.; Bushmaker, A.; Cronin, S. B. Radiation-induced direct bandgap transition in few-layer MoS2. *Appl. Phys. Lett.* **2017**, *111*, 131101.
(28) Foran, B.; Mann, C.; Peterson, M.; Bushmaker, A.; Wang, B.; Chen, J.; Yang, S.; Cronin, S. B. Effects of Proton Radiation-Induced Defects on Optoelectronic Properties of MoS2. *IEEE Trans. Nucl. Sci.* **2019**, *66*, 413−419.
(29) Sun, L.; Hu, H.; Zhan, D.; Yan, J.; Liu, L.; Teguh, J. S.; Yeow, E. K. L.; Lee, P. S.; Shen, Z. Plasma Modified MoS2Nanoflakes for Surface Enhanced Raman Scattering. *Small* **2014**, *10*, 1090−1095.
(30) Mouri, S.; Miyauchi, Y.; Matsuda, K. Tunable Photoluminescence of Monolayer MoS2 via Chemical Doping. *Nano Lett.* **2013**, *13*, 5944−5948.
(31) Li, Z.; Yang, S.; Dhall, R.; Kosmowska, E.; Shi, H.; Chatzakis, I.; Cronin, S. B. Layer Control of WSe2 via Selective Surface Layer Oxidation. *ACS Nano* **2016**, *10*, 6836−6842.
(32) Nan, H.; Wang, Z.; Wang, W.; Liang, Z.; Lu, Y.; Chen, Q.; He, D.; Tan, P.; Miao, F.; Wang, X.; Wang, J.; Ni, Z. Strong Photoluminescence Enhancement of MoS2through Defect Engineering and Oxygen Bonding. *ACS Nano* **2014**, *8*, 5738−5745.
(33) Kang, N.; Paudel, H. P.; Leuenberger, M. N.; Tetard, L.; Khondaker, S. I. Photoluminescence Quenching in Single-Layer MoS2 via Oxygen Plasma Treatment. *J. Phys. Chem. C* **2014**, *118*, 21258−21263.
(34) Yang, R.; Zheng, X. Q.; Wang, Z. H.; Miller, C. J.; Feng, P. X. L. Multilayer MoS2 transistors enabled by a facile dry-transfer technique and thermal annealing. *J. Vac. Sci. Technol. B* **2014**, *32*, 061203.
(35) Ganta, D.; Sinha, S.; Haasch, R. T. 2-D Material Molybdenum Disulfide Analyzed by XPS. *Surf. Sci. Spectra* **2014**, *21*, 19−27.
(36) Benson, E. E.; Zhang, H.; Schuman, S. A.; Nanayakkara, S. U.; Bronstein, N. D.; Ferrere, S.; Blackburn, J. L.; Miller, E. M. Balancing the Hydrogen Evolution Reaction, Surface Energetics, and Stability of Metallic MoS2 Nanosheets via Covalent Functionalization. *J. Am. Chem. Soc.* **2018**, *140*, 441−450.
(37) Yang, J.; Kim, S.; Choi, W.; Park, S. H.; Jung, Y.; Cho, M.-H.; Kim, H. Improved Growth Behavior of Atomic-Layer-Deposited High-k Dielectrics on Multilayer MoS2 by Oxygen Plasma Pretreatment. *ACS Appl. Mater. Interfaces* **2013**, *5*, 4739−4744.
(38) Khondaker, S. I.; Islam, M. R. Bandgap Engineering of MoS2 Flakes via Oxygen Plasma: A Layer Dependent Study. *J. Phys. Chem. C* **2016**, *120*, 13801−13806.
(39) Ma, W.; Alonso-González, P.; Li, S.; Nikitin, A.; Yuan, J.; Martín-Sánchez, J.; Taboada-Gutiérrez, J.; Amenabar, I.; Li, P.; Vélez, S.; Tollan, C.; Dai, Z.; Zhang, Y.; Sriram, S.; Kalantar-zadeh, K.; Lee, S.-T.; Hillenbrand, R.; Bao, Q. In-plane anisotropic and ultra-low-loss polaritons in a natural van der Waals crystal. *Nature* **2018**, *562*, 557.
(40) Huang, P.-R.; He, Y.; Cao, C.; Lu, Z.-H. Impact of lattice distortion and electron doping on α-MoO3 electronic structure. *Sci. Rep.* **2014**, *4*, 7131.